

O-MaMa @ EgoExo4D Correspondence Challenge: Learning Object Mask Matching between Egocentric and Exocentric Views

Lorenzo Mur-Labadia* Maria Santos-Villafranca* Alejandro Perez-Yus

Jesus Bermudez-Cameo Ruben Martinez-Cantin Jose J. Guerrero

I3A - University of Zaragoza

Abstract

The goal of the correspondence task is to segment specific objects across different views. This technical report re-defines cross-image segmentation by treating it as a mask matching task. Our method consists of: (1) A Mask-Context Encoder that pools dense DINOv2 semantic features to obtain discriminative object-level representations from FastSAM mask candidates, (2) an Ego \leftrightarrow Exo Cross-Attention that fuses multi-perspective observations, (3) a Mask Matching contrastive loss that aligns cross-view features in a shared latent space, and (4) a Hard Negative Adjacent Mining strategy to encourage the model to better differentiate between nearby objects.

1. Introduction

In the Ego-Exo4D [3] Correspondence task the goal is to predict an object’s mask in one perspective given a query mask from the other.

While the exocentric view captures both the full environment and the person’s body, it contains objects at multiple scales. Conversely, the egocentric view offers rich details on hand-object interactions, but it is highly dynamic, suffering from motion blur and frequent occlusions due to the ongoing interactions. These challenges make establishing precise object-level correspondences across views particularly difficult, requiring fine-grained segmentation and strong cross-view semantic reasoning.

We propose simplifying the complex cross-image segmentation task by reformulating it as Object Mask Matching (O-MaMa) across ego and exo views, leveraging the excellent zero-shot segmentation capabilities of Segment

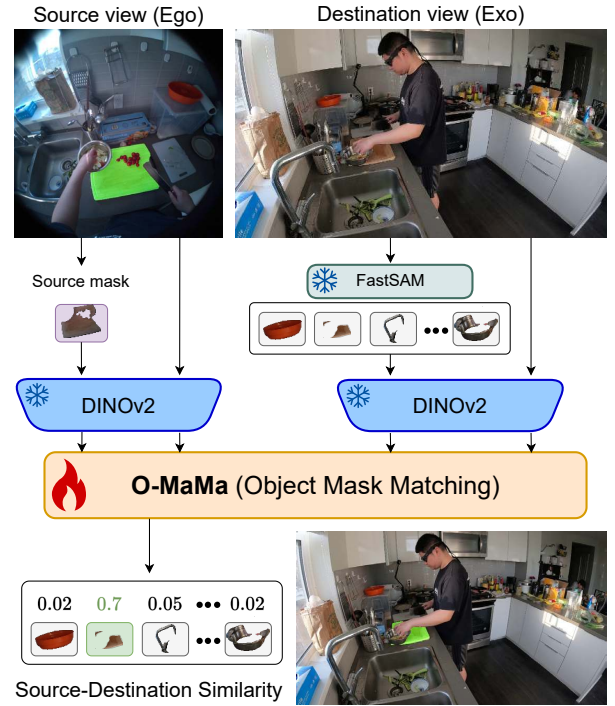


Figure 1. **Overview of our proposed Object Mask Matching (O-MaMa).** We obtain a set of mask candidates in the destination view using FastSAM. Through contrastive learning, we select the mask candidate that best matches the source mask.

Anything Models (SAM) [5]. An overview of our method is shown in Fig. 1. First, we extract a set of object mask candidates in the destination view using FastSAM [10]. To obtain mask descriptors, we encode each object mask with a *Mask-Context Encoder*, which pools dense DINOv2 [7] semantic features from both object masks and their extended bounding boxes, combining discriminative object features with contextual information. We introduce a *Hard Nega-*

*Equal contribution.

Corresponding authors: lmur@unizar.es,
m.santos@unizar.es

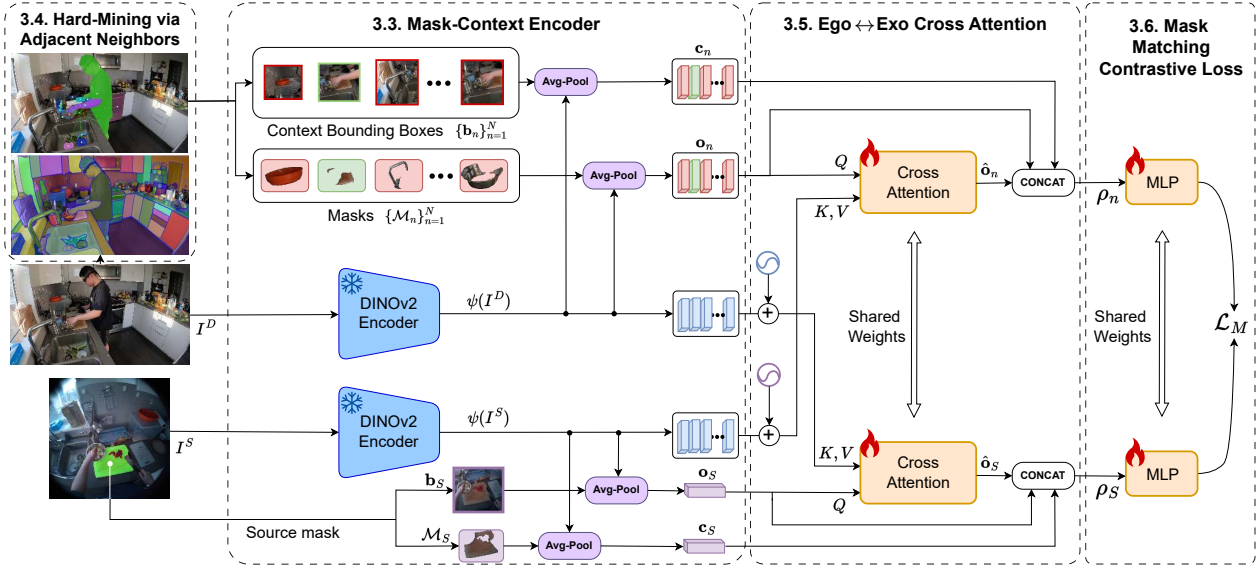


Figure 2. **O-MaMa architecture.** In the destination view, we generate a set of mask candidates with FastSAM. We extract descriptors on both source and destination masks by pooling dense DINOv2 features, and we aggregate global cross-view features with respective cross-attention mechanisms. We learn view-invariant features in a latent space via contrastive learning, and we select the most similar mask embedding to obtain the corresponding mask.



Figure 3. **Hard Negatives mining examples** We visualize 2^{nd} -order adjacent neighbors both in ego (left) and exo (right) scenarios.

tive Adjacent Mining strategy that selects neighboring object candidates to encourage the model to better differentiate between nearby objects. Next, we incorporate cross-view global features using a novel *Ego ↔ Exo Cross Attention* mechanism. Finally, we train the model with a *Mask Matching Contrastive Loss*, which selects the best mask candidate in the destination view by learning a cross-view feature alignment that captures both global scene context and fine-grained object features.

Our method is both simple and effective, achieving state of the art in the Ego-Exo4D Correspondence challenge (view Tab. 1). We obtain 42.6 (Ego2Exo) and 44.1 (Exo2Ego) IoU in the test v2 split, which represents a relative gain of +125.4% and +62.7% against the official challenge baselines [3], respectively.

2. Methodology

Fig. 2 shows the architecture of our method. The goal of O-MaMa is to select the object mask candidate in the destination view that matches the source mask best. Given a pair of images from two different views (egocentric and exocentric) and a query object mask \mathcal{M}_S in the source view I^S , the objective of the Ego-Exo Correspondences task is to predict the corresponding object mask in the destination view I^D . In the Ego2Exo task, the source view corresponds to the egocentric image, and the destination view is the exocentric image, and the opposite happens in the Exo2Ego setting.

We first extract a set of object mask proposals in the destination view using FastSAM [10], from which we compute object-level and contextual descriptors with the *Mask-Context Encoder* (Section 2.1). We also include cross-view global features through a novel *Ego ↔ Exo Cross Attention* mechanism (Section 2.3). We adopt a novel *Mask Matching Contrastive Loss* (Section 2.4) to learn view-invariant features by minimizing the distance between paired samples and maximizing the distance between negative (unpaired) samples in a shared latent space. During training, we enforce the model to learn more robust and discriminative object descriptors with a *Hard-Mining via Adjacent Neighbors* (Section 2.2).

2.1. Mask-Context Encoder

We first generate a set of dense mask proposals in the destination view using FastSAM [10], which segments intuitive

regions of the scene, such as entire objects, object parts or surfaces, with comparable quality to SAM [5], while being $50\times$ faster. Specifically, from the destination image, I^D , we generate N mask candidates $\{\mathcal{M}_n\}_{n=1}^N$.

Then, we compute a descriptor of each mask segment. We leverage DINOv2 [7], a self-supervised learning model, due to its high-level semantics, object decomposition capabilities and dense feature localization properties. We extract a local object descriptor $\mathbf{o}_n = \text{Avg-Pool}(\mathcal{M}_n, \psi(I^D))$ by pooling the corresponding object mask from the DINOv2 feature map of the destination image, denoted as $\psi(I^D)$. Some studies suggest [1, 2, 4] that humans leverage visual contextual associations among objects to represent scenes. Inspired by this, we extract a context descriptor $\mathbf{c}_n = \text{Avg-Pool}(\mathbf{b}_n, \psi(I^D))$ by pooling features from an extended bounding box \mathbf{B} around each mask. In both cases, we upsample $\times 4$ the DINOv2 feature map size in order to retain feature’s regions fine granularity [8]. Similarly, we extract object \mathbf{o}_S and context embeddings \mathbf{c}_S of the source mask \mathcal{M}_S in the other view.

2.2. Hard-Mining via Adjacent Neighbors

While the object embedding \mathbf{o}_n contains very discriminative object features, the context embedding \mathbf{c}_n incorporates surrounding information to help localizing the object in the other view, but this surrounding context also introduces ambiguity in cluttered environments, where nearby objects share a similar context. To address this, we introduce a hard-negative mining strategy based on adjacent neighbors, encouraging the model to disambiguate between nearby but distinct objects with similar context. In the destination view, we construct a graph of mask segments based on the pixel centers of each mask using the Delaunay Triangulation, as Fig. 3 shows. This results in a binary adjacency matrix $\mathcal{A} \in \{0, 1\}^{N \times N}$, defining the connectivity between segments. We define $\mathcal{N}(\mathbf{o}_n)$ to the set of neighbors of object \mathbf{o}_n . Then, we take the second order neighbor set $\mathcal{N}^2(\mathbf{o}_n) = \{\mathcal{N}(\mathbf{o}_j) \mid \forall \mathbf{o}_j \in \mathcal{N}(\mathbf{o}_n)\}$. Finally, we consider the joint set of first and second order neighbors as the hard negative candidates $\mathcal{O}_n^- = \{\mathcal{N}(\mathbf{o}_n) \cup \mathcal{N}^2(\mathbf{o}_n)\}$.

2.3. Ego↔Exo Cross Attention

Although the mask context embedding incorporates surrounding contextual information, it lacks a global representation across views. Therefore, we introduce a *Ego↔Exo Cross Attention* mechanism, which enhances the object embedding by extracting its corresponding semantic features in the other view. Specifically, we compute a cross attention operation [9] between the candidate object masks \mathbf{o}_n and the source image feature map $\psi(I^S)$.

$$\hat{\mathbf{o}}_n = \text{Softmax} \left(\frac{\mathbf{o}_n W_Q \cdot (\psi(I^S) W_K)^\top}{\sqrt{d}} \right) \cdot \psi(I^S) W_V$$

We compute query vectors from the candidate object descriptors \mathbf{o}_n with a linear projection W_Q , while key and value vectors represent the overall source image features $\psi(I^S)$ using the W_K and W_V linear layers. Before the cross-attention operation, we incorporate a learnable positional embedding to encode the spatial location of the patch tokens and a standard Layer Norm operation. Intuitively, the cross-view embedding of the object-mask candidates $\hat{\mathbf{o}}_n$ captures how each potential mask candidate is represented in the source view. Similarly, we compute the cross-view embedding of the source mask $\hat{\mathbf{o}}_S$ using the source mask descriptor \mathbf{o}_S for the queries and the overall destination image features $\psi(I^D)$ for the keys and values.

2.4. Mask Matching Contrastive Loss

The final descriptor ρ_n is obtained from the n -th candidate mask by concatenating its refined cross-view embedding $\hat{\mathbf{o}}_n$, the context embedding \mathbf{c}_n and the object embedding \mathbf{o}_n ; while the final descriptor ρ_S of the source mask is the result of concatenating $\hat{\mathbf{o}}_S$, \mathbf{c}_S and \mathbf{o}_S , respectively. Then, a shallow multi-layer perceptron $f_\theta(x) \in \mathbb{R}^{d_f}$ maps the cross-view embeddings to a latent feature representation, where d_f is the dimension of the common feature space. This mapping ensures that both egocentric and exocentric masks are embedded within a shared latent space, enabling a cross-view comparison.

Our contrastive loss is based on InfoNCE [6]. We select a batch \mathcal{B} of $|\mathcal{B}|$ elements, one positive and $|\mathcal{B}| - 1$ negatives from the list of closest neighbors around the target object in the other view \mathcal{O}_n^- as defined in Section 2.2. If the number of neighbors is greater than the negative batch size, $|\mathcal{O}_n^-| > |\mathcal{B}|$ we randomly select a subset of $|\mathcal{B}|$ elements from the neighbor set \mathcal{O}_n^- . If $|\mathcal{O}_n^-| < |\mathcal{B}|$ we also include masks from random objects from the rest of the image. If the number of segmented objects is less than the neighbor set \mathcal{O}_n^- , the objects are duplicated in order to fill the negative batch size $|\mathcal{B}|$. Finally, we apply the pairwise cosine similarity $\text{sim}(\cdot, \cdot)$ between the source mask embedding $f_\theta(\rho_S)$ and the batch of $|\mathcal{B}|$ mask candidates embeddings $\{f_\theta(\rho_n)\}_{n=1}^{|\mathcal{B}|}$ for computing the training loss:

$$\mathcal{L}_M(\rho^+, \rho_S) = -\log \frac{\exp(\text{sim}(f_\theta(\rho^+), f_\theta(\rho_S))/\tau)}{\sum_{n=1}^{|\mathcal{B}|} \exp(\text{sim}(f_\theta(\rho_n), f_\theta(\rho_S))/\tau)}$$

where $f_\theta(\rho^+)$ is the positive element in the batch. This *mask matching contrastive loss* aligns the corresponding cross-view object embeddings while it separates the remaining object candidates in the shared feature space.

2.5. Inference

At inference, we choose the object candidate whose embedding is closest to the source object in the latent space.

$$\mathcal{M}_{n^*}, \text{ where } n^* = \arg \max(\text{sim}[f_\theta(\rho_n), f_\theta(\rho_S)])$$

Method	Ego2Exo				Exo2Ego				Total-IoU↑
	IoU↑	Vis.A↑	Loc.E↓	Cont.A↑	IoU↑	Vis.A↑	Loc.E↓	Cont.A↑	
Baseline (XSegTx)	18.9	66.3	0.07	0.39	27.1	82.0	0.1	0.36	23.0
Ours (O-MaMa)	42.6	50.0	0.03	0.59	44.1	50.1	0.08	0.53	43.3

Table 1. Results on the EgoExo4D Correspondence Challenge test split.

Exp.	\mathcal{L}_M	Context	Adj. Neg	C.Attn	Global Union	Ego2Exo			Exo2Ego		
						IoU↑	Loc.E↓	Cont.A↑	IoU↑	Loc.E↓	Cont.A↑
Base.	-	-	-	-	-	35.2	0.191	0.455	34.9	0.163	0.423
A	✓	-	-	-	-	42.2	0.074	0.571	44.7	0.112	0.546
B	✓	✓	-	-	Concat	42.7	0.069	0.577	44.4	0.116	0.543
C	✓	✓	✓	-	Concat	46.9	0.079	0.599	45.6	0.107	0.548
D	✓	✓	✓	✓	Weighted Sum.	47.3	0.064	0.611	46.8	0.112	0.543
E	✓	✓	✓	✓	Concat	48.3	0.062	0.621	49.6	0.101	0.576
Relative Gain % of x with respect to y $\frac{(x-y)}{y}$						+37.2%	+67.5%	+36.5%	+42.1%	+38.0%	+36.2%

Table 2. Ablation study on the O-MaMa proposed modules on the validation set.

We use the source-destination similarity score to decide if the object is visible. Intuitively, if the object does not appear in the destination view, even the similarity of the closest object candidate should be low.

3. Results

3.1. Comparison with baseline of the challenge

Tab. 1 presents results on the v2 test set, demonstrating the our approach’s effectiveness. Our method, O-MaMa, improves performance, reaching 42.6 Ego2Exo and 44.1 Exo2Ego IoU, representing considerable relative gains¹ of up to +125.4% and +62.7% over XSegTx. The improvement is relatively consistent in the other segmentation metrics, where O-MaMa obtains 0.03 Loc.E, 0.59 Cont.A in the Ego2Exo task and 0.08 Loc.E and 0.53 Cont.A in the Exo2Ego task.

3.2. Ablation study.

O-MaMa architecture. Tab. 2 details the contribution of each O-MaMa component. Experiment A highlights the benefits of training a simple MLP with our novel Mask Matching Contrastive Loss \mathcal{L}_M , which aligns cross-view embeddings in a common latent space and improves IoU from 35.2 to 42.2 (Ego2Exo) and 34.9 to 44.7 (Exo2Ego). Second, Experiments A, B and C show that incorporating regional context is only beneficial when we sample adjacent negatives during training, as the hard-mining strategy forces the model to learn more fine-grained discriminative embeddings in nearby candidates with similar context but different mask descriptor. Next, our Ego↔Exo Cross Attention mechanism introduces cross-image content and global in-

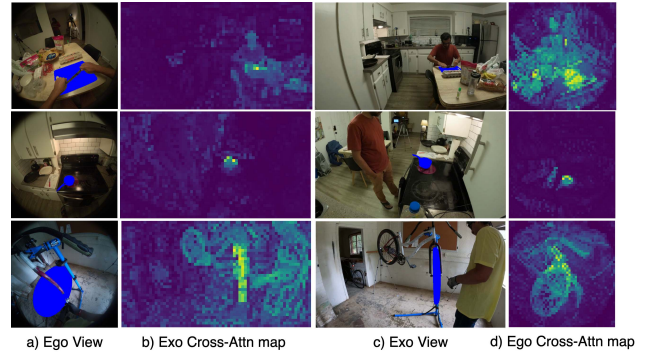


Figure 4. Ego↔Exo Cross-Attention maps

formation into the object embedding. As Fig. 4 shows, this module incorporates the object features from the other perspective, smoothing the cross-view alignment and improving the final performance. Finally, the joined effect of all our proposed modules specially improves the Loc.E, with relative improvements of +67.5% (Ego2Exo) and +38.0% (Exo2Ego), which yields a final gain of +37.2% Ego2Exo and +42.1% Exo2Ego IoU. This demonstrates that, while the model without any enhancements is agnostic to the candidate mask location (it just selects the most similar match), our proposed integration of local and global information results in an object mask selection more sensitive to the cross-view relationship.

3.3. Qualitative results

We show qualitative examples for the Ego2Exo (Fig. 7) and Exo2Ego (Fig. 5) tasks. The results show that top mask candidates are closely aligned due to their similar context, but our method correctly matches the top-1 mask candidate

¹We compute the relative gain% of x relative to y as $100 \cdot \left(\frac{x-y}{y}\right)$.



Figure 5. **Exo2Ego Qualitative Results.** We show the source mask in blue and the top 3 target masks in green, yellow and orange.

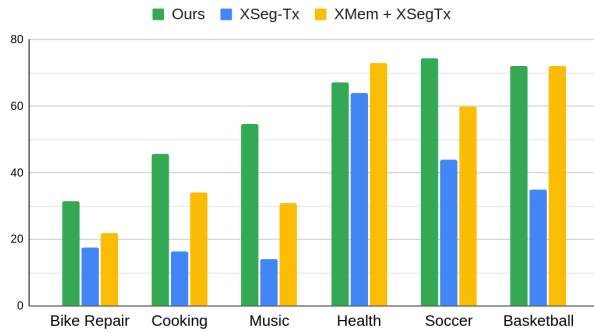


Figure 6. **Per-tasks Ego2Exo IoU performance.**

with the target object. FastSAM’s fine-grained zero-shot capabilities yield high-quality segmentation masks (*e.g.*, the *tire* in Fig. 7 and the *knife* or *bottle* in Fig. 5). However, as a limitation of our approach, they may produce partial segmentations when they capture only a part of the object (*e.g.*, the *saucepan* in Fig. 7). Finally, the total inference time of our approach is 250ms on average, of which 70ms correspond to the FastSAM mask extraction.

4. Conclusions

In this work, we address the problem of ego-exo object correspondences, a key step for multi-agent perception. We demonstrate that reformulating cross-view segmentation as an object mask matching problem simplifies the task while improving accuracy under zero-shot conditions. Our Mask Matching Contrastive Loss effectively aligns cross-view embeddings, while DINOv2 pooled mask features preserve fine-grained details. The proposed Hard Negative Adjacent Mining strategy enhances object differentiation, and Ego \leftrightarrow Exo Cross Attention integrates global cross-view context. As a result, O-MaMa achieves state-of-the-art performance on the EgoExo4D Correspondences task, obtaining a unified fine-grained segmentation and strong cross-view understanding.

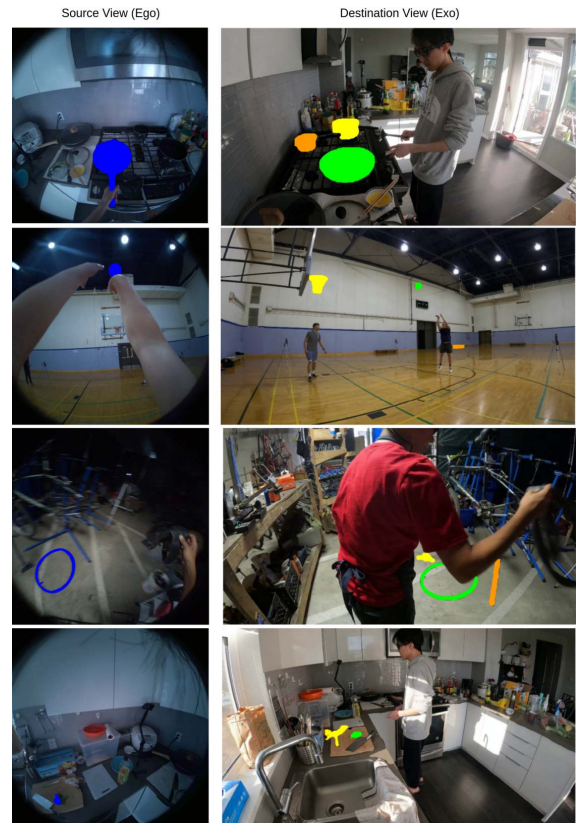


Figure 7. **Ego2Exo Qualitative Results.** For visualization purposes, we show the top 3 masks in green, yellow and orange.

References

- [1] Moshe Bar. Visual objects in context. *Nature Reviews Neuroscience*, 5(8):617–629, 2004. 3
- [2] Kartik Garg, Sai Shubodh Puligilla, Shishir Kolathaya, Madhava Krishna, and Sourav Garg. Revisit anything: Visual place recognition via image segment retrieval. In *European Conference on Computer Vision*, pages 326–343. Springer,

2024. [3](#)

- [3] Kristen Grauman, Andrew Westbury, Lorenzo Torresani, Kris Kitani, Jitendra Malik, Triantafyllos Afouras, Kumar Ashutosh, Vijay Baiyya, Siddhant Bansal, Bikram Boote, et al. Ego-exo4d: Understanding skilled human activity from first-and third-person perspectives. In *Proceedings of the IEEE/CVF Conference on Computer Vision and Pattern Recognition*, pages 19383–19400, 2024. [1](#), [2](#)
- [4] Helene Introub. The representation of visual scenes. *Trends in cognitive sciences*, 1(6):217–222, 1997. [3](#)
- [5] Alexander Kirillov, Eric Mintun, Nikhila Ravi, Hanzi Mao, Chloe Rolland, Laura Gustafson, Tete Xiao, Spencer Whitehead, Alexander C Berg, Wan-Yen Lo, et al. Segment anything. In *Proceedings of the IEEE/CVF international conference on computer vision*, pages 4015–4026, 2023. [1](#), [3](#)
- [6] Aaron van den Oord, Yazhe Li, and Oriol Vinyals. Representation learning with contrastive predictive coding. *arXiv preprint arXiv:1807.03748*, 2018. [3](#)
- [7] Maxime Oquab, Timothée Darcet, Théo Moutakanni, Huy Vo, Marc Szafraniec, Vasil Khalidov, Pierre Fernandez, Daniel Haziza, Francisco Massa, Alaaeldin El-Nouby, et al. DINOv2: Learning robust visual features without supervision. *arXiv preprint arXiv:2304.07193*, 2023. [1](#), [3](#)
- [8] Michal Shlapentokh-Rothman, Ansel Blume, Yao Xiao, Yuqun Wu, Sethuraman TV, Heyi Tao, Jae Yong Lee, Wilfredo Torres, Yu-Xiong Wang, and Derek Hoiem. Region-based representations revisited. In *Proceedings of the IEEE/CVF Conference on Computer Vision and Pattern Recognition*, pages 17107–17116, 2024. [3](#)
- [9] Ashish Vaswani, Noam Shazeer, Niki Parmar, Jakob Uszkoreit, Llion Jones, Aidan N Gomez, Łukasz Kaiser, and Illia Polosukhin. Attention is all you need. *Advances in neural information processing systems*, 30, 2017. [3](#)
- [10] Xu Zhao, Wenchao Ding, Yongqi An, Yinglong Du, Tao Yu, Min Li, Ming Tang, and Jinqiao Wang. Fast segment anything. *arXiv preprint arXiv:2306.12156*, 2023. [1](#), [2](#)